OPEN ACCESS
JOURNAL OF ADVANCED DIELECTRICS
Vol. 11, No. 1 (2021) 2150008 (11 pages)

DOI: 10.1142/S2010135X21500089

Synthesis of novel PANI-based Ti(IV) phosphosulphosalicylate composite cation exchanger — structural, electrical, and impedance properties

T. Amutha*,‡ and K. Jacinth Mispa†

*Aditanar College of Arts and Science, Tiruchendur-628 216
Affiliating to Manonmaniam Sundaranar University, Abishekapatti
Tirunelveli-627 012, Tamil Nadu, India

†Department of Chemistry, Aditanar College of Arts and Science
Tiruchendur-628 216, Affiliating to Manonmaniam Sundaranar University
Abishekapatti, Tirunelveli-627 012, Tamil Nadu, India

‡tamutha1982@gmail.com

Received 19 January 2021; Revised 16 February 2021; Accepted 17 February 2021; Published 18 March 2021

In order to combine the properties of inorganic ion exchanger and conducting organic polymer, a new class of organic–inorganic composite cation exchanger PANI–Ti(IV) phosphosulphosalicylate (PTPSS) was synthesized by intercalating polyaniline (PANI) into Ti(IV) phosphosulphosalicylate (Ti(IV) PSS) using sol–gel chemical route with enhanced properties. PTPSS has been characterized by using Fourier Transform Infrared Spectroscopy (FT-IR), X-ray diffraction (XRD), Scanning Electron Microscopy (SEM), Energy dispersive X-ray (EDAX), thermo gravimetric analysis (TGA-DTG), and Transmission Electron Microscopy (TEM). Ac electrical conductivity studies were also performed. This material possessed electrical conductivity of $10^{-3}-10^{-6}$ Scm^{-1} which falls in the semiconducting range. The frequency ($2\times10^{5}-1\times10^{6}$ Hz) dependent Ac conductivity at room temperature suggests the evidence for the transport mechanism for the conductivity in PTPSS. The structure of the composite cation exchanger extremely supports its conducting behavior.

Keywords: Polyaniline–Ti(IV) phosphosulphosalicylate; composite cation exchanger; electrical conductivity; transport mechanism; impedance studies.

1. Introduction

"Organic–inorganic" electrically conducting polymer-based composite cation exchanger can be produced by the combination of organic conducting polymers into the polyvalent metal acid salts of inorganic precipitates.[1] PANI is considered as the most interesting conducting polymer due to its specialities such as low cost monomer, good environmental stability, high electrical conductivity, ease of synthesis, and remarkable redox properties linked with the nitrogen chain.[2] An interesting property of polyaniline is the reversibly tunable redox characteristics in which the electrical conductivity is controlled by protonation and charge-transfer doping while compared to other conjugated organic polymers.[3] High conducting composite systems have been used in biosensors,[4] electromagnetic interference (EMI) shielding,[5] electrode for rechargeable lithium batteries, and separators in high power and smart windows.[6] PANI is the only conducting organic polymer whose properties depend on many factors such as oxidation state, protonation state/doping level, and nature of dopants. The conductivity of the polyaniline increases due to the protonation of mineral acids.[7] Nanoparticles such as Ag,[8] Ni,[9] MnO_2,[10] SnO_2,[11] and TiO_2,[12] etc. could act as conductive dopants between the PANI chains that are responsible for the improvement in the electrical conductivity of nanocomposites. Poly-o-toluidine Th(IV) phosphate was synthesized by sol–gel technique has the conductivity in the range of 10^{-2} to 10^{-3} S/cm.[6] Poly-o-toluidine Zr(IV) phosphate was synthesized by sol–gel method, possessed DC electrical conductivity in the semiconducting range.[13] Polyaniline Sn(IV) phosphate shows excellent conducting behavior within the semiconducting range.[14] Nanocomposites of poly-o-toluidine and Thorium(IV) phosphate have excellent conducting behavior which is employed in electrochemical application.[15] To investigate the impedance characteristics of poly (o-anisidine) with TiO_2 particles, carbon black and MWNT were deposited in a thin film which is used for biosensing application.[16] PANI-based Ti(IV) phosphosulphosalicylate (PTPSS) composite cation exchanger was synthesized and structural characterization done by using different instrumental techniques is explained in the present work.

*Research Scholar, Register Number: 18122022032001.

2. Experimental Procedure

2.1. *Materials*

Aniline, potassium persulphate (KPS), Ti(IV) chloride, sodium phosphate, and sulphosalicylic acid were used for the synthesis of composite cation exchanger PTPSS. All the chemicals and reagents used in this work are of analytical grade and used as such.

2.2. *Synthesis of composite cation exchanger PTPSS*

2.2.1. *Preparation of the reagents*

0.1 M Ti(IV) chloride was prepared using 0.1 M HCl. 0.05 M sodium phosphate and 0.05M sulphosalicylic acid were prepared using demineralized water. 0.1 M aniline and 0.1 M potassium persulphate were prepared using 1 M HCl.

2.2.2. *Synthesis of polyaniline emeraldine salt*

The mechanism for the formation of polyaniline and the nature of its structure has been summarized in Scheme 1. Polyaniline emeraldine salt was synthesized by the oxidative polymerization of aniline[17] using potassium persulphate as an oxidizing agent (Scheme 2). Polymerization was effected by the dropwise addition of 0.1 M $K_2S_2O_8$ (oxidant) to the continuously stirred solution of 0.1 M aniline in 1 M HCl for 20 min. After the addition of KPS, polymerization was allowed to proceed and the green color gel of polyaniline

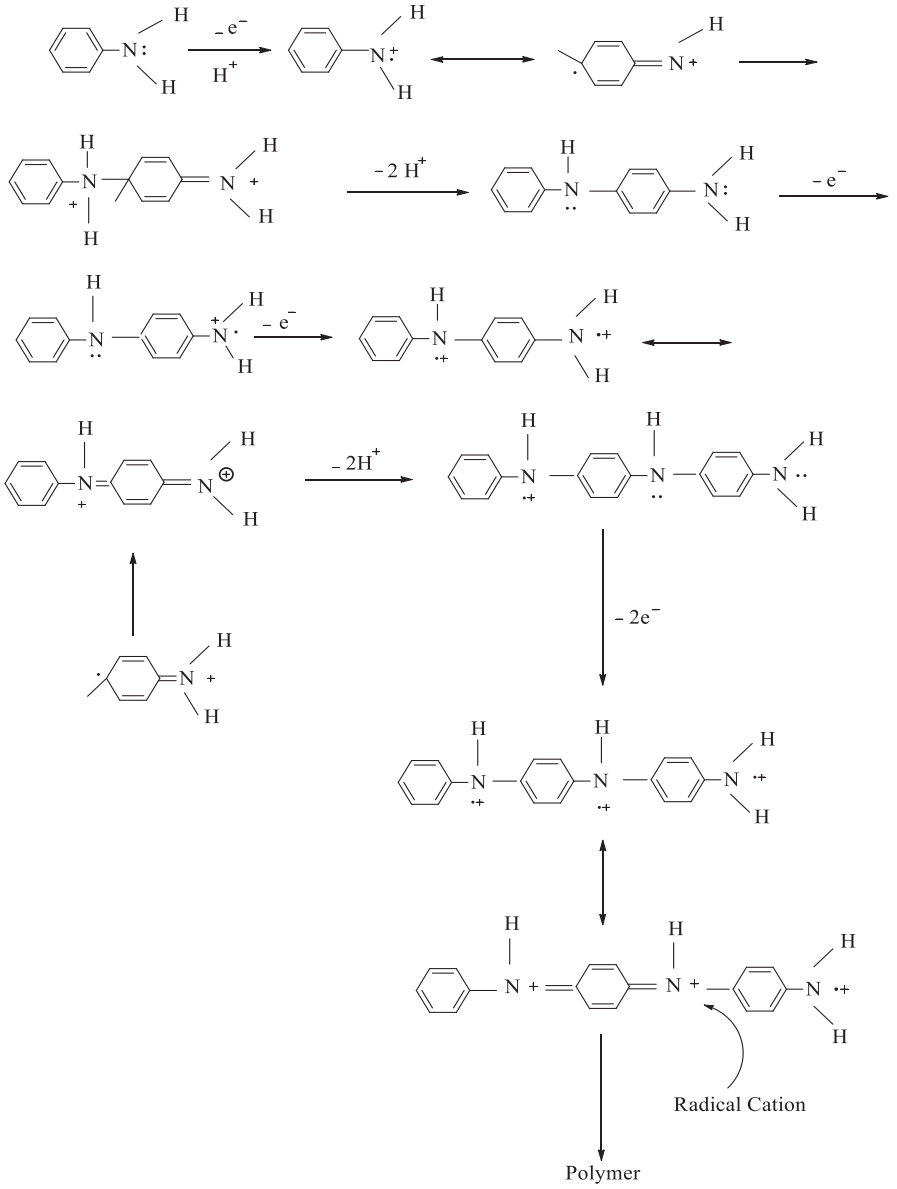

Scheme 1. Reaction mechanism for radical cation coupling of aniline leading to the formation of a linear polyaniline polymer.

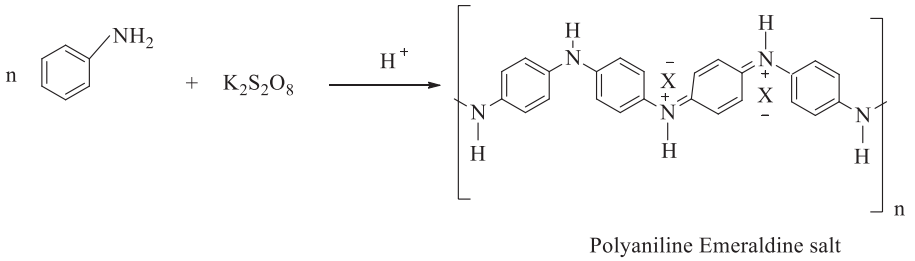

Scheme 2. Mechanism for the synthesis of polyaniline emeraldine salt.

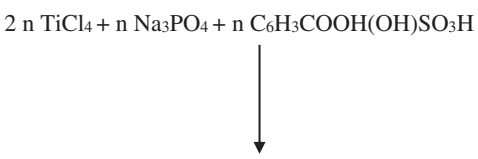

Scheme 3. Formation of Ti(IV) PSS.

was obtained when it was kept overnight in refrigerator.[18] The precipitated polyaniline emeraldine salt was filtered and washed with distilled water, pure ethanol, and finally with acetone to remove the oligomers. It was dried at 60 °C in an oven for about 4 h and the dried polymer sample was powdered in a mortar.

2.2.3. *Synthesis of Ti(IV) phosphosulphosalicylate (Ti(IV) PSS) inorganic ion exchanger*

Ti(IV) phosphosulphosalicylate (Ti(IV) PSS)[19] was prepared by adding a solution of Ti(IV) chloride in 0.1 M HCl solution which was added to the mixture of sulphosalicylic acid and sodium phosphate in the molar ratio 2:1:1. The solution obtained was allowed to settle at room temperature for 24 h, filtered and washed with demineralized water repeatedly. The formation of Ti(IV) PSS has been given in Scheme 3.

2.2.4. *Synthesis of composite cation exchanger PTPSS*

The composite cation exchanger was prepared by the sol–gel mixing of polyaniline emeraldine salt into the inorganic ion exchanger Ti(IV)PSS. In this method, the gels of polyaniline emeraldine salt were added to the white colored inorganic precipitate of Ti(IV) PSS with a constant stirring for 3 h. The resultant mixture was turned slowly into greenish black colored slurries. The resultant greenish black colored slurries were kept in refrigerator for 24 h. Now the gels of composite cation exchanger PTPSS were filtered off and washed thoroughly with ethanol and acetone to remove the impurities and KPS and dried in an oven at 60 °C. They were converted into H^+ form by treating with 0.1 M HNO_3 for 24 h with occasional shaking and washed several times with deionized water in order to remove the excess acid and then dried at 50 °C.

3. Characterization

The polymer samples were characterized by Fourier transform infrared (FT-IR) spectrophotometer (Thermo Nicolet Avatar 370), X-ray diffractrometer (Bruker AX8 D8 Advance Twin), Scanning electron microscope (JEOL-JSM-6390 LV), energy dispersive X-ray studies (OXFORD XMX N), Thermo gravimetric analysis (Perkin Elmer STA 6000 instrument), and Transmission electron microscopy (JEOL/TEM 2100). Dielectric and impedance spectrum measurements were performed by using impedance analyzer-IM6 ZAHNER.

The frequency-dependent Ac electrical conductivity of the composite cation exchanger PTPSS can be calculated by using the following equations.

$$\sigma_{ac} = 2\pi f \varepsilon \ \varepsilon_r \tan\delta, \tag{1}$$

$$\varepsilon_r = C/C, \tag{2}$$

$$C_0 = A\varepsilon_0/d, \tag{3}$$

$$A = \pi r \tag{4}$$

where σ_{ac} is the ac electrical conductivity, A is the area of the sample (m^2), d is the thickness of the sample (m), r is the radius of the sample (m), ε_0 is the permittivity in free space (8.85×10^{-12} f/m), ε_r is the relative permittivity, C is the capacitance at particular temperature (f), C_0 is the capacitance at absolute temperature (f), f is the frequency (Hz), and tan δ is the loss tangent.

4. Results and Discussion

4.1. *Reaction mechanism*

Different organic–inorganic composite cation exchangers have been prepared by adding the transition metal ions (e.g., Zr, Ti, V, Mo, Cr, Sc, Sn, and As) into the organic framework matrix.[20] Titanium-supported hybrid materials were established because they have advantages over other

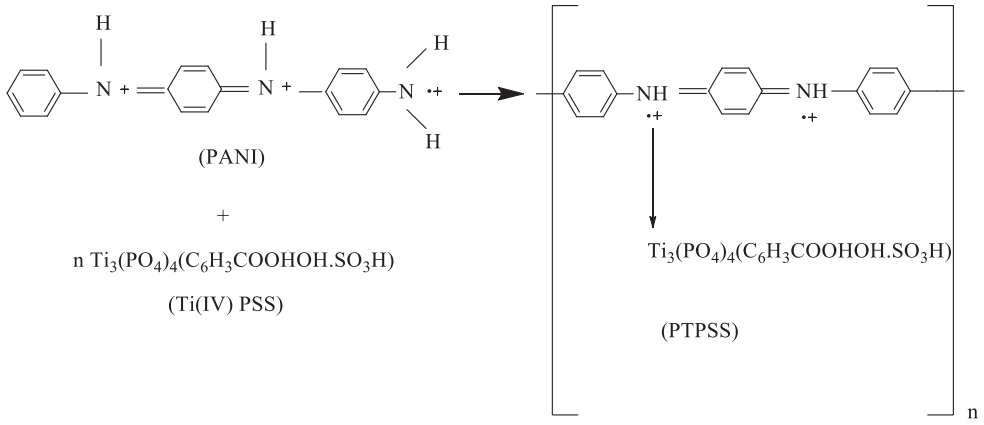

Scheme 4. Mechanism for the formation of composite cation exchanger PTPSS.

composite cation exchangers. The mechanism for the formation of composite cation exchanger PTPSS has been given in Scheme 4.

4.2. *Fourier transform infrared (FT-IR) analysis*

The FT-IR spectra of Ti(IV) PSS, PANI–Cl^-, and PTPSS are shown in Fig. 1. In the FT-IR spectrum of Ti(IV) PSS, peaks at 3414, 1628, 1384, 1029, 804, 626, and 470 cm^{-1} were attributed to the presence of hydroxyl groups and interstitial water, C=O stretching vibration of carboxylic acid group, characteristic for benzene ring, sulphonate group, phosphate group, and Ti–O stretching vibration, respectively (Fig. 1(a)).[21] The FT-IR spectrum of polyaniline emeraldine salt shows that the peaks observed at 3423, 2918, 1562, 1479, 1298 and 1252 cm^{-1} were due to the N–H stretching vibration of the amine group, CH_2 stretching vibration, C=C stretching vibration of the quinonoid ring, stretching vibration of C=C of the benzenoid ring, C–N stretching vibration, and C=N stretching vibrations, respectively (Fig. 1(b)).[22]

The FT-IR spectrum of composite cation exchanger PTPSS (Fig. 1(c)) shows that the peak at 3472 cm^{-1} due to the stretching vibration of secondary amine, the peak at 3016 cm^{-1} corresponds to the CH_2 stretching vibration, the peak at 1697 cm^{-1} related to the C=C stretching vibration of the quinonoid ring, the peak at 1399 cm^{-1} shows that the stretching vibration of C=C of the benzenoid ring, the peak at 1316 cm^{-1} due to the C–N stretching vibration, the peak at 1248 cm^{-1} due to the C=N stretching vibrations. The FT-IR spectrum of composite cation exchanger PTPSS shows that the change in intensity of characteristic peaks in PTPSS compared to Ti(IV) PSS and PANI–Cl^- which clearly indicated the binding of polyaniline with the inorganic counterpart (Ti(IV) PSS) of composite cation exchanger.

4.3. *X-ray diffraction (XRD) analysis*

The XRD pattern of Ti(IV) PSS, PANI–Cl^-, and PTPSS are shown in Fig. 2. The XRD pattern of PANI–Cl^- shows the

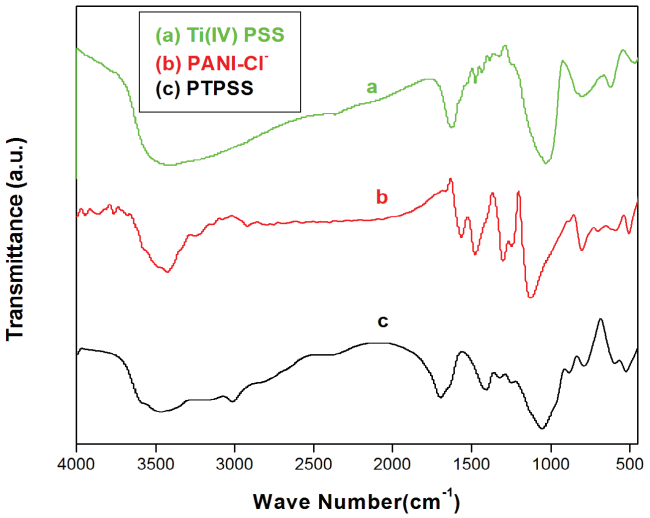

Fig. 1. FT-IR spectra of (a) Ti(IV) PSS, (b) PANI-Cl^-, and (c) PTPSS.

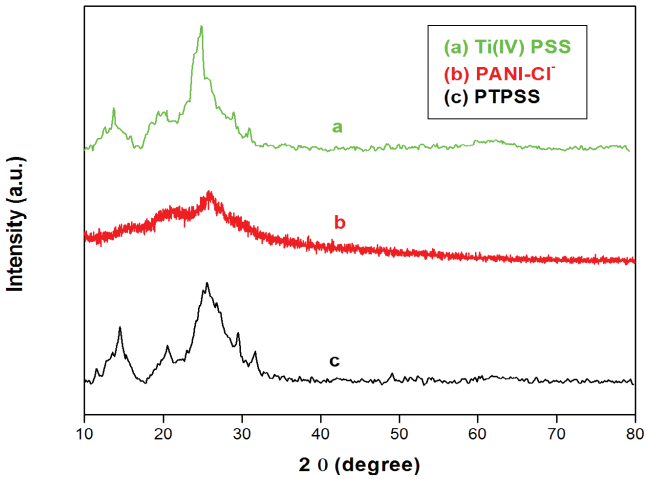

Fig. 2. XRD pattern for (a) Ti(IV) PSS, (b) PANI–Cl^-, and (c) PTPSS.

broad diffraction peak, attributed to amorphous nature of polyaniline emeraldine salt and $2\theta \sim 25°$ indicates the characteristic peak for polyaniline[23] (Fig. 2(b)). XRD pattern of composite cation exchanger PTPSS (Fig. 2(c)) indicates that the polycrystalline nature of the PTPSS. This suggests that the crystalline nature of composite cation exchanger is changed after the binding of inorganic ion exchanger Ti(IV) PSS with PANI matrix.

The average crystallite size was calculated by using the well-known Debye–Scherrer's equation as follows:

$$D = 0.96\lambda / \beta \cos\theta , \quad (5)$$

where D is the average crystallite size in nanometer, λ is the X-ray wavelength in angstroms, β is the full width at half maximum in radians, and θ is the Bragg's angle in degree.[24] The average crystallite size was found to be 20, 29, and 23 nm for PANI–Cl^-, Ti(IV) PSS, and PTPSS, respectively.

K is a dimensionless shape factor with a value close to unity. The shape factor has a typical value of about 0.9, but varies with the actual shape of the crystallite. K depends on the definitions of the average crystallite size and in the absence of detailed shape information, $K = 0.9$ is a good approximation.[25,26] The as-synthesized composite cation exchanger PTPSS is a polymer-based material. In polymer-based material, particular symmetric crystal is not present.

Some of the polyaniline-based materials 0.9–0.96 is used for K in the Debye–Scherrer's equation.

Some of the references are added here. 0.9 is used by Prasanna *et al.*,[27] 0.94 is used by Mannu *et al.*,[28] Ranjini *et al.*[29] and Dubey *et al.*[30] used 0.96 for K value. Mispa *et al.*[31] used the value as 0.9 to 1 and Mispa *et al.*[32] also used 0.96 for K in the Debye–Scherrer's equation.

4.4. *Scanning electron microscopy (SEM) analysis*

Figure 3 shows that the SEM images of composite cation exchanger PTPSS at different magnifications indicating the binding of inorganic ion exchanger i.e., Ti(IV) PSS with organic polymer i.e., PANI–Cl^-. It has been revealed that after binding of PANI–Cl^- with Ti(IV) PSS, the morphology has been changed. It is seen from the SEM images of composite cation exchanger PTPSS, the surface of the inorganic ion exchanger Ti(IV) PSS was uniformly covered by the organic polymer. Thus, the organic conducting polymer

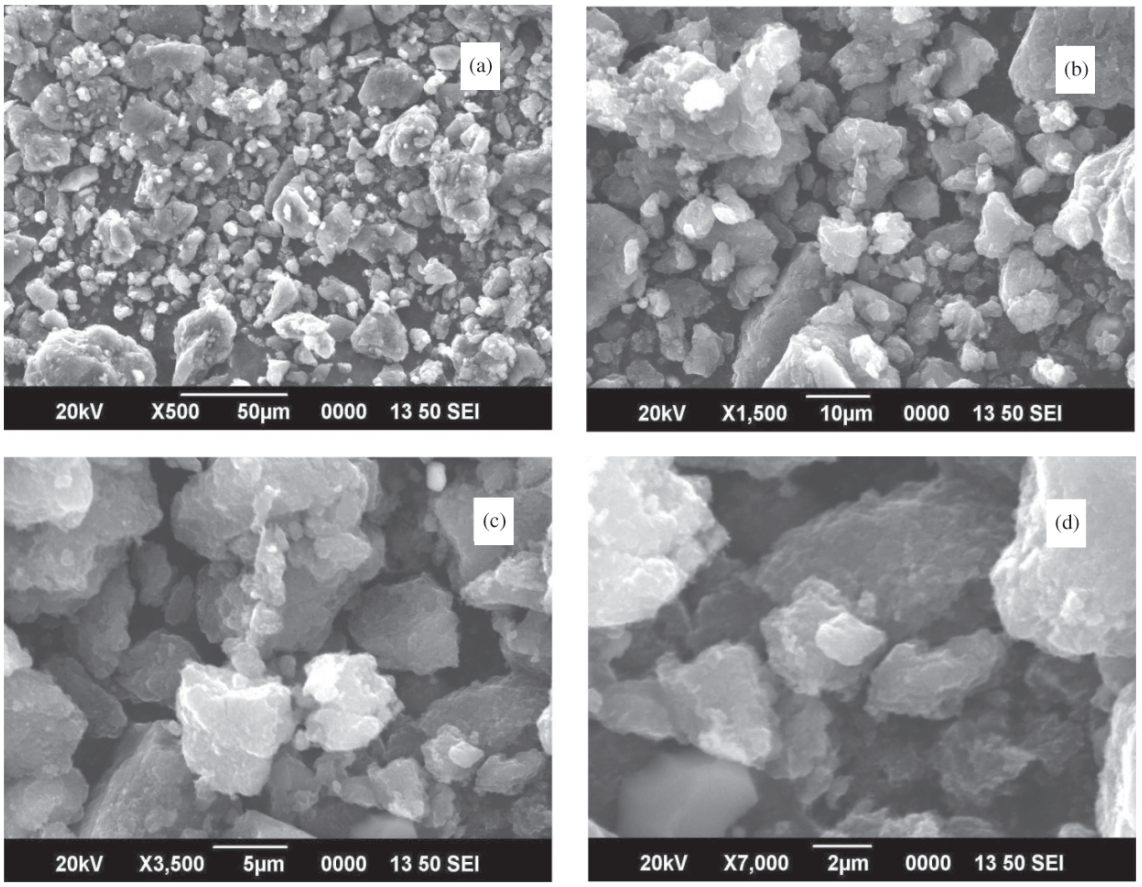

Fig. 3. SEM images of composite cation exchanger PTPSS at different magnifications.

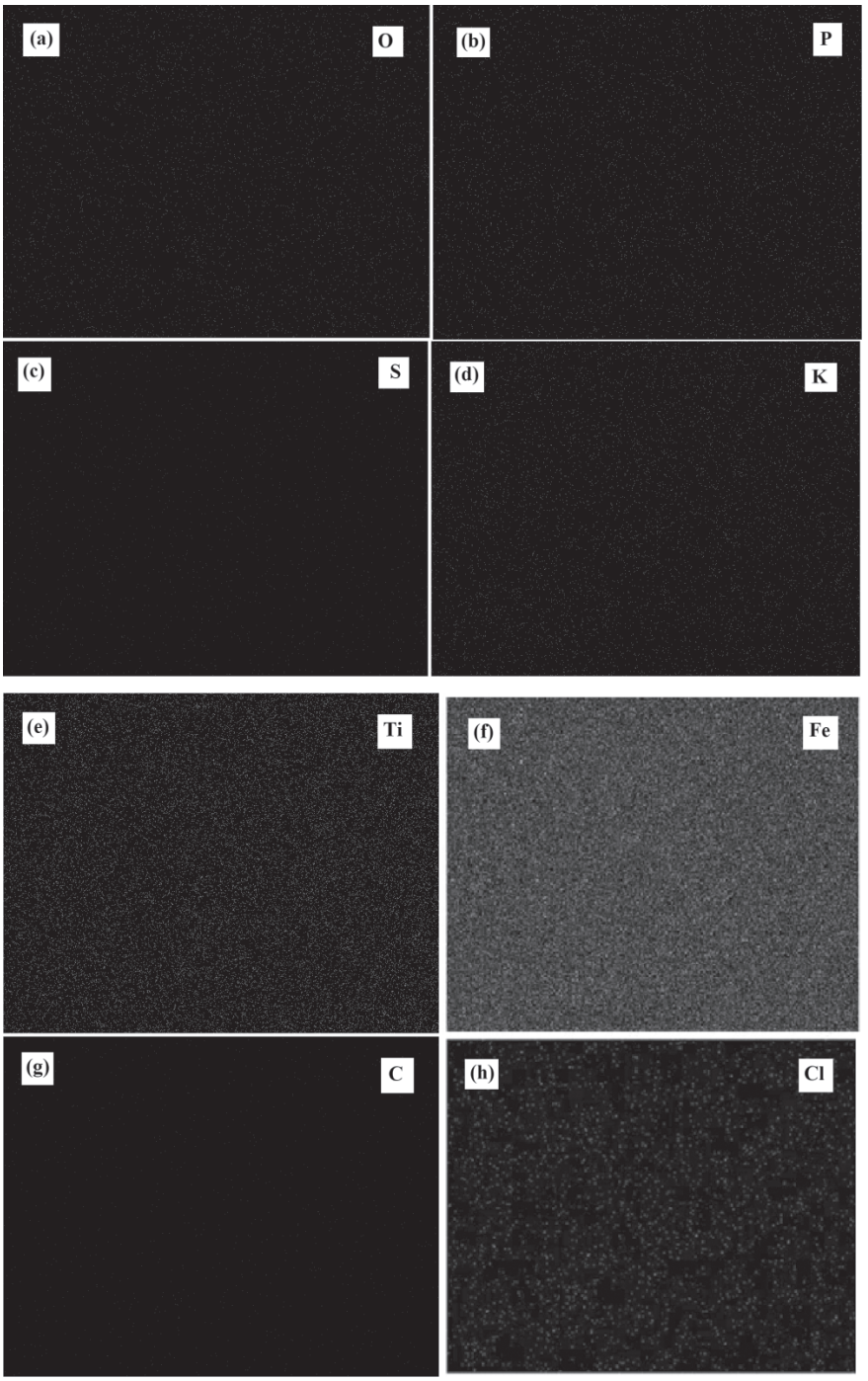

Fig. 4. EDAX element mapping for (a) O, (b) P, (c) S, (d) K, (e) Ti, (f) Fe, (g) C, and (h) Cl.

is tightly binding to the inorganic ion exchanger providing mechanical stability.

4.5. *Chemical composition (EDAX) analysis*

The EDAX analysis was helpful to examine the incorporation of inorganic ion exchanger into the PANI matrix (Fig. 4). The EDAX confirms that Ti(IV) PSS were effectively incorporated into PANI matrix. The composition of the elements present in the composite cation exchanger PTPSS is presented in Table 1.

4.6. *Thermal analysis*

TGA studies of PANI–Cl^-, Ti(IV) PSS, and PTPSS in nitrogen atmosphere are shown in Figs. 5 and 6, respectively.

Table 1. Elemental composition of PTPSS from EDAX.

Element	wt.%	at.%
C	77.53	85.67
O	13.19	10.94
P	0.3	0.13
S	1.65	0.68
Cl	5.69	2.13
K	0.25	0.09
Ti	0.78	0.22
Fe	0.61	0.15
Total	100	100

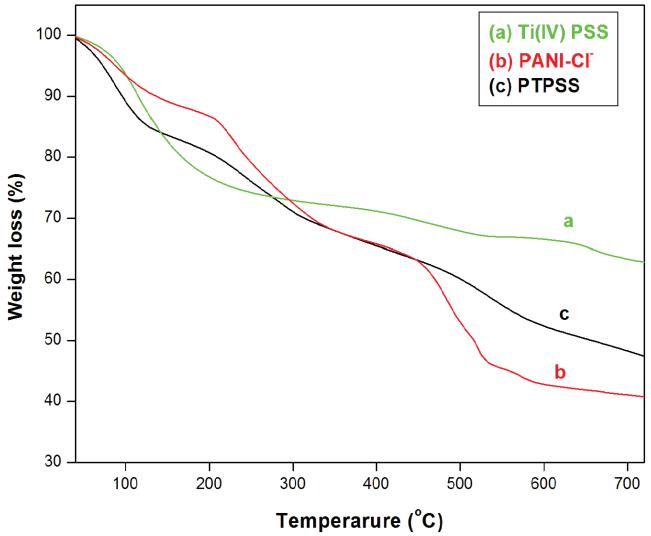

Fig. 5. TGA curve of (a) Ti(IV) PSS, (b) PANI–Cl⁻, and (c) PTPSS.

From the TGA curve of Ti(IV) PSS (Fig. 5(a)) a sharp weight loss up to 100°C can be attributed to the loss of external water molecule. The weight loss in the region of 100–350 °C may be due to the condensation of –OH groups and also accompanied by the loss of sulphosalicylic acid by vaporization. The weight loss between 350 °C and 600 °C may be due to the condensation of –OH groups and it is accompanied by the loss of phosphorous. A constant weight after 600 °C seems to be the formation of stable metal oxides.[21]

From the TGA curve of PANI–Cl⁻ (Fig. 5(b)), the initial weight loss up to 150 °C is due to the elimination of water molecule and the next weight loss from 200 °C is due to the decomposition of polyaniline. Then, the polymer degrades rapidly above 600 °C.[33] From the TGA curve of PTPSS (Fig. 5(c)), the loss in weight up to 100 °C is due to the removal of external water molecule. The weight loss from

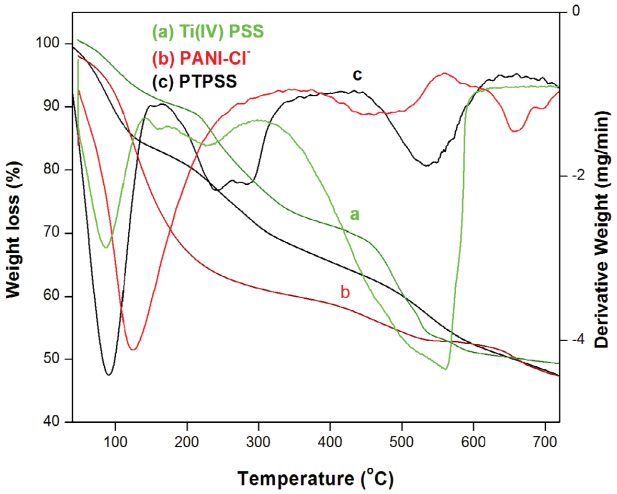

Fig. 6. Simultaneous TGA-DTG curve of (a) Ti(IV) PSS, (b) PANI-Cl⁻, and (c) PTPSS.

200 °C to 500 °C is due to the elimination of the dopant molecule. Above 500 °C, there is a complete decomposition of PANI matrix. From TGA studies, it is inferred that the composite cation exchanger PTPSS has better thermal stability compared to PANI–Cl⁻ emeraldine salt.

4.7. *Transmission electron microscopy (TEM) analysis*

From TEM micrograph, the particle size of composite cation exchanger PTPSS is in nano range i.e., in the range of 40–66 nm as shown in Fig. 7, which proves that the prepared composite cation exchanger PTPSS is a nanocomposite material.

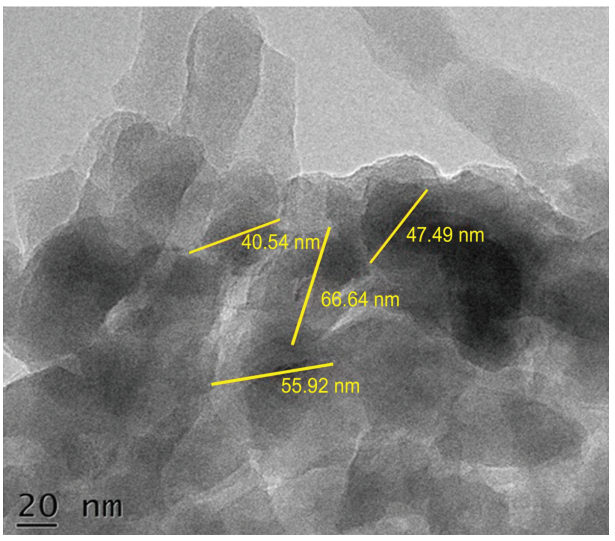

Fig. 7. TEM images of composite cation exchanger PTPSS.

Table 2. Ac electrical conductivity of Ti(IV) PSS, PANI–Cl⁻, and PTPSS.

Sample	σ_{ac} (Scm$^{-1)}$
Ti(IV) PSS	8.04×10^{-6}
PANI–Cl⁻ (emeraldine salt)	5.89×10^{-3}
PTPSS	6.58×10^{-3}

4.8. *Measurement of Ac electrical conductivity*

The frequency-dependent Ac electrical conductivity of Ti(IV) PSS, PANI–Cl⁻ (emeraldine salt), and composite cation exchanger PTPSS are given in Table 2.

From the above table, it was clearly indicated that the Ac electrical conductivity of the composite cation exchanger PTPSS is higher than that of the PANI–Cl⁻ (emeraldine salt). The improvement in Ac electrical conductivity for composite cation exchanger PTPSS is due to the effective dispersion of Ti(IV) PSS in the PANI matrix which favors better electronic transport. It was found that the value of Ac electrical conductivity for the composite cation exchanger PTPSS lie in the order of 10^{-3}–10^{-6} Scm^{-1} which is in the semiconductor range.

The frequency-dependent Ac electrical conductivity of composite cation exchanger PTPSS in the frequency range $2 \times 10^5 - 1 \times 10^6$ Hz is also studied. It shows that the Ac electrical conductivity is frequency dependent and enhances with increase in frequency. The charge carriers are transported between the polymer chains of the defect sites by hopping process. So the Ac electrical conductivity of composite cation exchanger PTPSS increases as frequency increases. Oxidation of the polymer at high level gives bipolaron and the oxidation of the polymer at lower level gives polarons. In the conjugated system of the polymer, polarons and bipolarons move along the polymer chains due to the single and double bonds rearrangement.[34] The mechanism of conduction in the composite cation exchanger PTPSS is explained by the polaron and bipolaron formation. The charge transport mechanism in polymer with nondegenerate ground state is determined by the conduction of polarons and bipolarons. The number of charge carriers available for conduction and their mobility i.e., the rate at which they move are used to determine the magnitude of the conductivity.[35] The molecular alignment of the chains within the entire system also affects the electrical conductivity which explains the correlation between the structure and conductivity of the polymer.

Figure 8 shows the Ac conductivity of the composite cation exchanger PTPSS at different frequencies at room temperature. The composite cation exchanger PTPSS exhibit the frequency-independent behavior in the region of low frequency and then increased in the region of high frequency. At high frequency region, the Ac conductivity increases because of the formation of excess charge carriers polarons and bipolarons in that region.

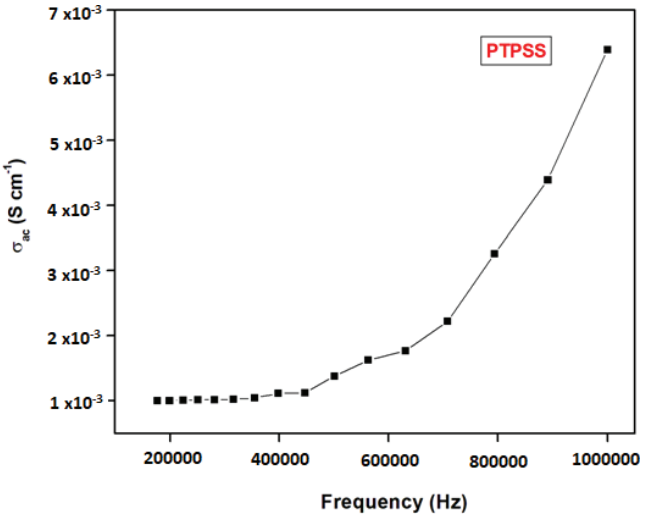

Fig. 8. Frequency-dependent σ_{ac} conductivity of PTPSS.

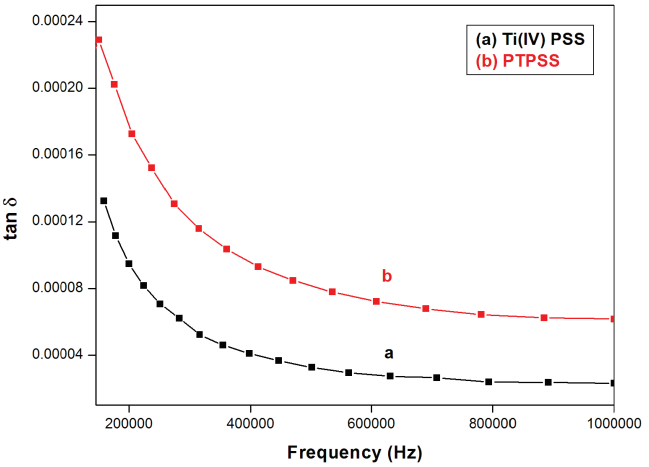

Fig. 9. Frequency dependence on dissipation factor of PTPSS.

In PTPSS, polyaniline facilitating the charge carrier motion decreases the resistance and increases the conductivity.[36]

4.9. *Dielectric properties*

The dielectric properties have been studied for the composite cation exchanger PTPSS. Loss tangent variation with frequency for PTPSS is shown in Fig. 9 and loss tangent decreases with increase in frequency and at the higher frequency region the loss tangent becomes almost constant and the similar behavior was observed by Inamdar *et al.*[37]

Figure 10 shows the variation of dielectric constant (ε') as a function of frequency (f) for composite cation exchanger PTPSS. It shows that with the increase in frequency, the dielectric constant decreases and becomes

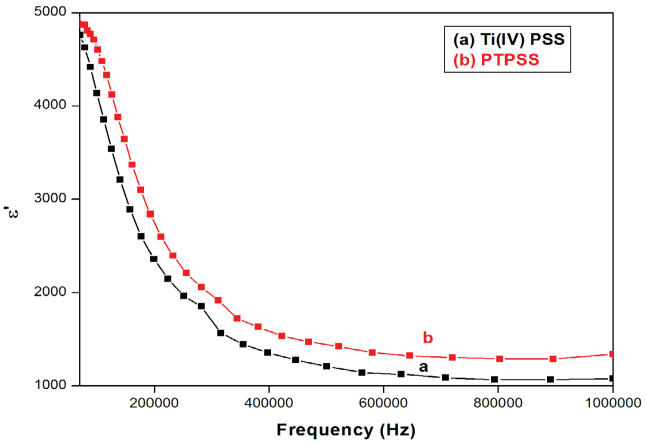

Fig. 10. Frequency dependence of dielectric constant of PTPSS.

almost constant at higher frequencies. The obtained high dielectric constant values at lower frequencies are related to the effects of space charge polarization.[38] The term space charge polarization depends on the availability of free charge carriers and conductivity of the composite cation exchanger. Therefore, space charge polarization plays an important role in the composite cation exchanger PTPSS. The dielectric constant is considered as frequency dependent having larger values at lower frequencies. As polaron and bipolaron are moveable, it moves along the polymer chain of the composite cation exchanger PTPSS. Therefore, it acts as a semiconductor. When frequency increased, the present dipoles cannot reorient automatically. So, the dielectric constant is decreased.[39]

From the Ac electrical conductivity studies it was revealed that the dielectric constant (ε') and dissipation factor (tan δ) exhibit the normal dielectric behavior and decrease with the increase in frequency. Therefore, the structure can support the electrical properties of this composite cation exchanger PTPSS.

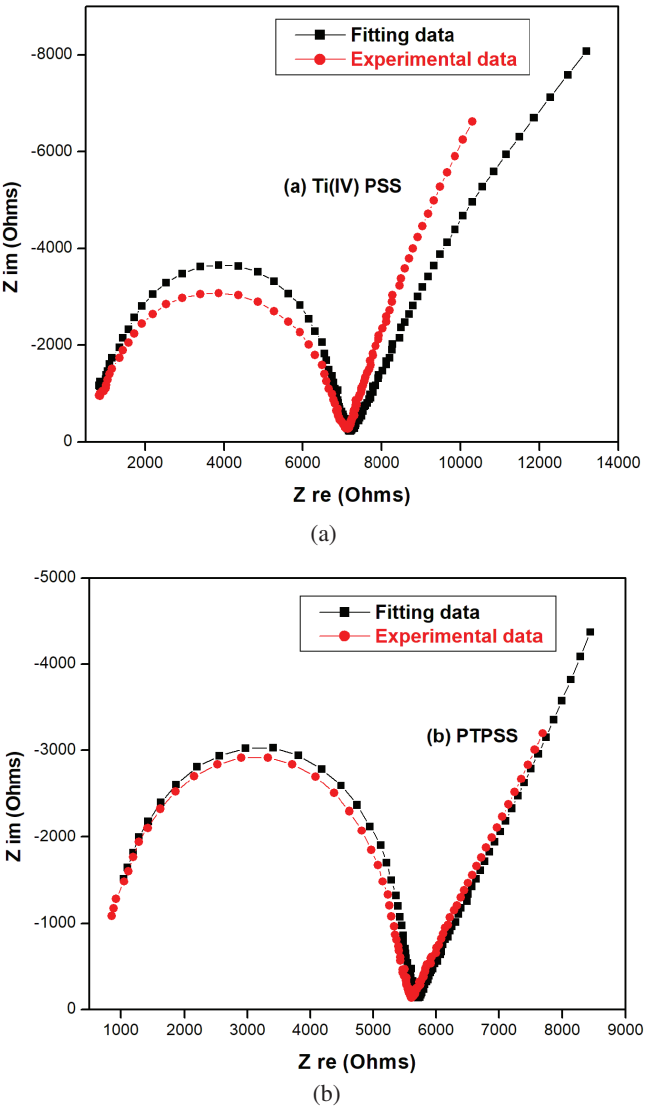

Fig. 11. Nyquist plots and their corresponding fitted curves for (a) Ti(IV) PSS and (b) PTPSS.

4.10. *Impedance studies*

Impedance spectroscopy is a powerful technique for characterizing the electrical properties of the composite cation exchanger as a function of frequency to understand their complete relaxation and conduction mechanism. Plotting the imaginary part Z'' against the real part Z' (Nyquist plot) on a linear scale that yields semicircles based on the nature of composite cation exchanger under consideration. Based on the theoretical models there are three semicircles observed on the Nyquist plot, high frequency region semicircle represents the bulk contribution, in the intermediate frequency region it represents the grain boundary or interface contribution, and the lowest frequency region it represents polymer electrode contribution.[40] Figure 11 illustrates that the Nyquist plots for Ti(IV) PSS and PTPSS and their corresponding fitted curves. The Nyquist plot is consisted of a distorted semicircle in the region of high frequency and nearly a vertical line along the imaginary axis at region of low frequency. The smaller semicircle denotes the excellent electrical conductivity and the lowest resistance value of the composite cation exchanger.[41] In the low frequency region, composite cation exchanger PTPSS shows more ideal capacitor behavior.[42]

From Bode plots, magnitude of impedance and phase angle can be noted. From the plot, resistance and double layer capacitance are clearly seen on the Y-axis. Figure 12 shows the Bode plot for Ti(IV) PSS and PTPSS. The phase angle of PTPSS was about −52°, exhibiting nearly pure capacitive behavior.[27] At low frequencies, the sloping lines declare the capacitive behavior of the composite cation exchanger PTPSS.

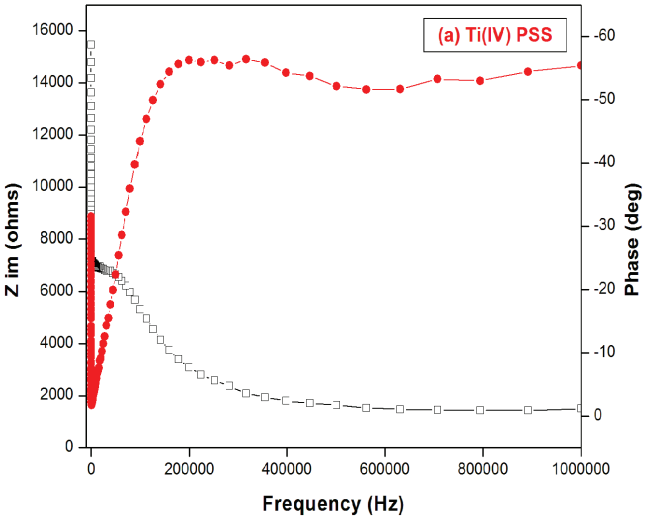

(a)

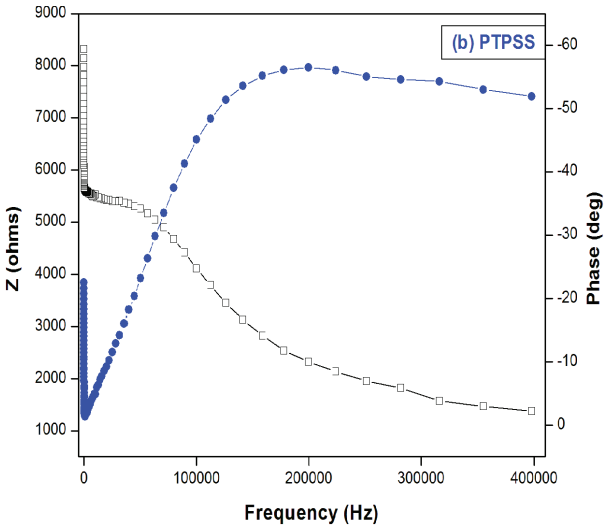

(b)

Fig. 12. Bode plot for (a) Ti(IV) PSS and (b) PTPSS.

5. Conclusion

In the present study, electrically conducting polymeric–inorganic composite cation exchanger PTPSS with novel structure was synthesized by sol–gel method. Fourier transform infrared spectral analysis was used to identify various functional groups present in the composite cation exchanger PTPSS. Various elements present in the composite cation exchanger PTPSS were identified by EDAX analysis. The results of FT-IR and XRD have provided a clear evidence about the formation of PANI–Ti(IV) PSS. Conduction in composite cation exchanger PTPSS is predominantly performed by variable range hopping process. Thus, the polarons acts as charge carriers hopping from state to state in polymer samples. Electrical conductivity and structural studies result indicate that the composite cation exchanger PTPSS can be employed in sensors and in ion exchange membranes.

Acknowledgments

We are thankful to the Research Department of Chemistry, Aditanar College of Arts and Science, Tiruchendur for providing necessary research facilities. This research did not receive any specific grant from funding agencies in the public, commercial, or not-for-profit sectors.

References

[1]A. A. Khan, Inamuddin and M. M. Alam, Preparation, characterization and analytical applications of a new and novel electrically conducting fibrous type polymeric-inorganic composite material: Polypyrrole Th(IV) phosphate used as a cation-exchanger and Pb(II) ion-selective membrane electrode, *Mater. Res. Bull.* **40**, 289 (2004). doi:10.1016/j.materresbull.2004.10.014.

[2]E. Detsri and S. T. Dubas, Interfacial polymerization of polyaniline and its layer-by-layer assembly into polyelectrolytes multilayer thin-films, *J. Appl. Polym. Sci.* **128**, 558 (2013). doi:10.1002/app.38168.

[3]A. Kaur, A. Kaur and D. Saini, A review on synthesis of silica nanocomposites with conducting polymers: Polyaniline, *Int. J. Eng. Sci.* **18**, 40 (2016).

[4]Z. M. Tahir, E. C. Alocilja and D. L. Grooms, Polyaniline synthesis and its biosensor application, *Biosens. Bioelectron.* **20**, 1690 (2005). doi:10.1016/j.bios.2004.08.008.

[5]K. Lakshmi, H. John, K. T. Mathew, R. Joseph and K. E. George, Microwave absorption, reflection and EMI shielding of PU–PANI composite, *Acta Mater.* **57**, 371 (2009). doi:10.1016/j.actamat.2008.09.018.

[6]A. A. Khan and A. Khan, Electrical conductivity and cation exchange kinetic studies on poly-o-toluidine Th(IV) phosphate nano-composite cation exchange material, *Talanta* **73**, 850 (2007). doi:10.1016/j.talanta.2007.05.003.

[7]R. Murugesan and E. Subramanian, Charge dynamics in conducting polyaniline–metal oxalate composites, *Bull. Mater. Sci.* **26**, 529 (2003). doi:10.1007/BF02707352.

[8]Y. Jin and M. Jia, Preparation and electrochemical capacitive performance of polyaniline nanofiber-graphene oxide hybrids by oil–water interfacial polymerization, *Synth. Met.* **189**, 47 (2014). doi:10.1016/j.synthmet.2013.12.016.

[9]C. Bora, A. Kalita, D. Das, S. K. Dolui and P. Kr. Mukhopadhyay, Preparation of polyaniline/nickel oxide nanocomposites by liquid/liquid interfacial polymerization and evaluation of their electrical, electrochemical and magnetic properties, *Polym. Int.* **63**, 445 (2013). doi:10.1002/pi.4522.

[10]J. G. Wang, Y. Yang, Z. H. Huang and F. Kang, Interfacial synthesis of mesoporous MnO_2/polyaniline hollow spheres and their application in electrochemical capacitors, *J. Power Sources* **204**, 236 (2012). doi: 10.1016/j.jpowsour.2011.12.057.

[11]G. D. Khuspe, S. T. Navale, M. A. Chougule, S. Sen, G. L. Agawane, J. H. Kim and V. B. Patil, Facile method of synthesis of polyaniline-SnO2 hybrid nanocomposites: Microstructural, optical and electrical transport properties, *Synth. Met.* **178**, 1 (2013). doi:10.1016/j.synthmet.2013.06.022.

[12]A. Katoch, M. Burkhart, T. Hwang and S. S. Kim, Synthesis of polyaniline/TiO_2 hybrid nanoplates via a sol–gel chemical method, *Chem. Eng. J.* **192**, 262 (2012). doi:10.1016/j.cej.2012.04.004.

[13]A. A. Khan and T. Akhtar, Preparation, physico-chemical characterization and electrical conductivity measurement studies of an organic–inorganic nanocomposite cation-exchanger:

Poly-o-toluidine Zr(IV) phosphate, *Electrochim. Acta* **53**, 5540 (2008). doi:10.1016/j.electacta.2008.03.002.

[14]A. A. Khan and Inamuddin, Preparation, physico-chemical characterization, analytical applications and electrical conductivity measurement studies of an 'organic–inorganic' composite cation-exchanger: Polyaniline Sn(IV) phosphate, *React. Funct. Polym*. **66**, 1649 (2006). doi:10.1016/j.reactfunctpolym.2006.06.007.

[15]A. A. Khan, A. Khan and Inamuddin, Preparation and characterization of a new organic–inorganic nano-composite poly-o-toluidine Th(IV) phosphate: Its analytical applications as cation-exchanger and in making ion-selective electrode, *Talanta* **72**, 699 (2007). doi:10.1016/j.talanta.2006.11.044.

[16]S. Carrara, V. Bavastrello, D. Ricci, E. Stura and C. Nicolini, Improved nanocomposite materials for biosensor applications investigated by electrochemical impedance spectroscopy, *Sens. Actuators B* **109**, 221 (2005). doi:10.1016/j.snb.2004.12.053.

[17]Mu. Naushad, Z. A. Al-Othman and M. Islam, Adsorption of cadmium ion using a new composite cation-exchanger polyaniline Sn(IV) silicate: Kinetics, thermodynamic and isotherm studies, *Int. J. Environ. Sci. Technol*. **10**, 567 (2013). doi:10.1007/s13762-013-0189-0.

[18]Z. A. Al-Othman, Mu. Naushad and A. Nilchi, Development, characterization and ion exchange thermodynamics for a new crystalline composite cation exchange material: Application for the removal of Pb^{2+} ion from a standard sample (Rompin Hematite), *J. Inorg. Organomet. Polym*. **21**, 547 (2011). doi:10.1007/s10904-011-9491-9.

[19]R. Thomas, Synthesis, properties and analytical applications of Titanium (IV) phosphosulphosalicylate - A new hybrid inorganic-organic ion-exchanger, *Orient. J. Chem*. **24**, 139 (2008).

[20]M. Shahadat, T. T. Teng, M. Rafatullah and M. Arshad, Titanium-based nanocomposite materials: A review of recent advances and perspectives, *Colloids Surf. B* **126**, 121 (2015). doi:10.1016/j.colsurfb.2014.11.049.

[21]D. K. Singh and S. Singh, Synthesis, characterization and analytical applications of zirconium(IV) sulphosalicylophosphate, *Indian J. Chem. Technol*. **11**, 23 (2004).

[22]G. D. Prasanna and H. S. Jayanna, In situ synthesis, characterization and frequency dependent AC conductivity of polyaniline/$CoFe_2O_4$ nanocomposites, *J. Adv. Dielectr*. **1**, 357 (2011). doi:10.1142/s2010135x11000434.

[23]A. Khan, A. M. Asiri, M. A. Rub, N. Azum, A. A. P. Khan, S. B. Khan, M. M. Rahman and I. Khan, Synthesis, characterization of silver nanoparticle embedded polyaniline tungstophosphate-nanocomposite cation exchanger and its application for heavy metal selective membrane, *Compos. Part B* **45**, 1486 (2013). doi:10.1016/j.compositesb.2012.09.023.

[24]M. Khairy, R. Kamal, N. H. Amin and M. A. Mousa, Kinetics and isotherm studies of Remazol Red adsorption onto polyaniline/cerium oxide nanocomposites, *J. Bas. Environ. Sci*. **3**, 123 (2016).

[25]H. P. Klug and L. E. Alexander, *X-Ray Diffraction Procedures*, 2nd edn., Chapter 9 (Wiley, 1974).

[26]B. D. Cullity, *Elements of X-ray Diffraction*, 2nd edn. (Addison-Wesley, 1978)

[27]B. P. Prasanna, D. N. Avadhani, H. B. Muralidhara, K. Chaitra, V. R. Thomas, M. Revanasiddappa and N. Kathyayini, Synthesis of polyaniline/ZrO_2 nanocomposites and their performance in AC conductivity and electrochemical supercapacitance, *Bull. Mater. Sci*. **39**, 667 (2016). doi:10.1007/s12034-016-1196-9.

[28]P. Mannu, M. Palanisamy, G. Bangaru, S. Ramakrishnan, A. Kandasami and P. Kumar, Temperaturedependent AC conductivity and dielectric and impedance properties of ternary In–Te–Se nanocomposite thin films, *Appl. Phys. A*. **458**, 125 (2019). doi:10.1007/s00339-019-2751-1.

[29]P. S. P. Ranjini, V. S. John and R. Murugesan, Synthesis, characterization and anti-microbial activities on polyaniline-$CdTiO_3$ nanocomposite, *J. Pharm. Chem. Biol. Sci.* **5**, 221 (2017).

[30]H. K. Dubey and P. Lahiri, Synthesis, structural, dielectric and magnetic properties of Cd^{2+} based Mn nanosized ferrites, *Mater. Technol*. 36, 131 (2020).

[31]K. J. Mispa, P. Subramaniam and R. Murugesan, Studies on polyaniline/ silver molybdate nanocomposites, *Int. J. Nanosci*. 13, 1450002 (2014).

[32]K. J. Mispa, P. Subramaniam and R. Murugesan, Oxidative polymerization of Aniline using Zirconium Vanadate, a novel Polyaniline hybrid ion exchanger, *Des. Monomers Polym.* **14**, 423 (2011). doi:10.1163/138577211X587627.

[33]L. Ding, X. Wang and R. V. Gregory, Thermal properties of chemically synthesized polyaniline EB powder, *Synth. Met*. **104**, 73 (1999). doi:10.1016/s0379-6779(99)00035-1.

[34]Z. A. Al. Othman, M. M. Alam, Mu. Naushad and R. Bushra, Electrical conductivity and thermal stability on polyaniline Sn(IV) tungstomolybdate nanocomposite cation-exchange material: Application as Pb(II) ion-selective membrane electrode, *Int. J. Electrochem. Sci*. **10**, 2663 (2015).

[35]G. Sharma, D. Pathania and Mu. Naushad, Preparation, characterization, and ion exchange behavior of nanocomposite polyaniline zirconium(IV) selenotungstophosphate for the separation of toxic metal ions, *Ionics* **21**, 1045 (2015). doi:10.1007/s11581-014-1269-y.

[36]S. Palsaniya, H. B. Nemade and A. K. Dasmahapatra, Graphene based PANI/MnO_2 nanocomposites with enhanced dielectric properties for high energy density materials, *Carbon* **150**, 179 (2019). doi:10.1016/j.carbon.2019.05.006.

[37]H. K. Inamdar, M. Sasikala, S. B. Chakradhar, B. Sannakki and M. V. N. Ambikaprasad, AC conductivity studies of polyaniline/CuO composites, *Indian J. Sci. Res*. **17**, 30 (2017).

[38]V. Kathiravan, G. Satheesh Kumar, S. Pari and P. Selvarajan, Influence of dye doping on the structural, spectral, optical, thermal, mechanical and nonlinear optical properties of L-Histidine hydrofluoride dehydrate crystals, *J. Mol. Struct*. **1223**, 128958 (2020). doi:10.1016/j.molstruc.2020.128958.

[39]J. Hazarika and A. Kumar, Electric modulus based relaxation dynamics and ac conductivity scaling of polypyrrole nanotubes, *Synth. Met*. **198**, 239 (2014). doi:10.1016/j.synthmet.2014.10.009.

[40]K. S. Hemalatha, G. Sriprakash, M. V. N. Ambikaprasad, R. Damle and K. Rukmani, Temperature dependent dielectric and conductivity studies of polyvinyl alcohol-ZnO nanocomposites films by impedance spectroscopy, *J. Appl. Phys*. **118**, 154103 (2015). doi:10.1063/1.4933286.

[41]H. Gul, A. A. Shah, U. Krewer and S. Bilar, Study on direct synthesis of energy efficient multifunctional polyaniline–graphene oxide nanocomposite and its application in aqueous symmetric supercapacitor devices, *Nanomaterials* **10**, 118 (2020). doi:10.3390/nano10010118.

[42]K. Shen, F. Ran, X. Zhang, C. Liu, N. Wang, X. Niu, Y. Liu, D. Zhang, L. Kong, L. Kang and S. Chen, Supercapacitor electrodes based on nano-polyaniline deposited on hollow carbon spheres derived from cross-linked co-polymers, *Synth. Met*. **209**, 369 (2015). doi:10.1016/j.synthmet.2015.08.012.